

Atmospheric effects on high-velocity impact cratering in porous sandstones

Shachi Singh^{1*}, Brett Kuwik², Justin Moreno² and Ryan Hurley^{1,2**}

¹Department of Mechanical Engineering, Johns Hopkins University, Baltimore, MD, USA

²Hopkins Extreme Materials Institute, Johns Hopkins University, Baltimore, MD, USA

Abstract. Granular geomaterials feature varied porosity and may possess pore fluids. The interactions between grains, pores, and pore fluids affect the impact dynamics in the material such as the cratering efficiency, ejecta kinetics and crater morphology. In this study, we conduct experimental analyses of high-velocity projectile impacts on sandstone to understand the effect of porosity and air pressure on the behaviour of porous geomaterials during impact. Our results show that different target porosities feature separate trends in crater morphology: Impact under air pressure results in larger crater diameters in low porosity sandstone but smaller crater diameters in sandstone of higher porosity. These results further highlight the significance of studying the relationship between grains, gas and pore spaces to understand the evolution of failure in porous rocks.

1 Introduction

Impact events in geomaterials cause significant changes in the structural and material properties around the site of impact. The study of impact craters in porous geomaterials is important in planetary sciences and defense applications. Porosity and pore fluids play an important role in the cratering process in granular targets under impact [1-5]. However, the correlation between grain packing, interstitial fluid, and the response of the material, remains unclear.

Prior studies have demonstrated the effects of pore saturation on the impact process in porous rocks [3][4]. Shultz [6] reported that the atmospheric pressure and grain sizes play a more important role in influencing the cratering efficiency in loose, fine-grained beds than the material properties of the target. Royer et al. [7] observed a dual effect of interstitial air on impact response of granular beds: the presence of air enhanced projectile penetration in loosely packed beds but hindered it in denser ones. Their observations suggest that this variation occurs due to the resistance to change in packing density offered by the interstitial air in the granular bed.

The current work seeks to examine this interplay of porosity and atmospheric pressure on cratering in porous rocks. We specifically examine the hypothesis that the dual effect of interstitial air on impact response observed by Royer et al. [7] is also observed

in porous rocks. To test this hypothesis, we conducted a series of impact experiments on sandstones of two porosities at low and high atmospheric pressures.

2 Methodology

2.1 Target Material

The target materials are Bentheimer or Nugget sandstone cylinders measuring 3 inches in diameter and 4 inches in length, shown in Fig. 1. Bentheimer sandstone has a density of 2.1 g/cm³, a manufacturer's P50 grain size of 0.208 mm, and 24.5% porosity. Nugget sandstone has a density of 2.4 g/cm³, a manufacturer's P50 grain size of 0.147 mm, and 11% porosity. Through separate high-resolution image analysis, our Bentheimer and Nugget sandstones had measured P50s of 0.204 mm and 0.109 mm, respectively [8]. Fig. 2a. and 2b. show the microstructures of Bentheimer and Nugget sandstones, respectively, highlighting the difference in porosities of the two samples. The similar mineral composition and differing porosities of these two sandstones allow for an examination of impact behaviour as a function of sample porosity.

2.2 Experimental Set-up

The impact experiments were conducted at the Hopkins Extreme Materials Institute, using the Hypervelocity

* email: ssing155@jh.edu

** email: rhurley6@jhu.edu

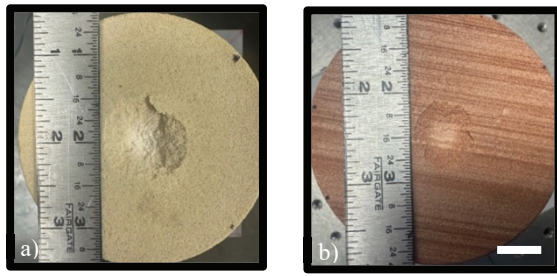


Fig. 1. Cratered sandstone target cylinders post-impact: a) Bentheimer b) Nugget

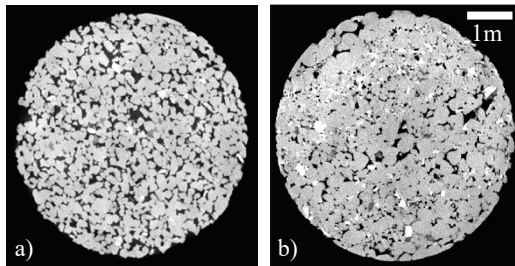


Fig. 2. X-ray tomography of sandstone microstructures: a) Bentheimer b) Nugget

Facility for Impact Research Experiments (HyFIRE). HyFIRE is a two-stage light gas gun that can launch projectiles at velocities up to 7 km/s [9] (Fig. 3a). The cylindrical target is setup inside the chamber, with circular face perpendicular to the direction of impact (Fig. 3b). Projectiles were 3 mm Aluminum spheres impacting at 2 km/s. The atmospheric pressure in the target chamber was varied from 50 torr to 700-760 torr. Three in-situ diagnostic methods were used: high-speed video imaging at 1 million fps, orthogonal flash X-ray imaging, and laser sheets for ejecta tracking. The video imaging parallel and perpendicular to the impact face of the cylinders allowed visualization of the transient crater formation and the ejecta cloud. Experimental conditions are listed in Table. 1.

2.3 Post Impact Analysis

Post-impact damage analysis was conducted using 3D X-ray micro-computed tomography (μ CT) to analyse the crater morphology and examine the impact-induced damage in the targets. The scans were performed using an RX Solutions EasyTom 160, using a 150 kV X-ray source. First, we scanned the samples before impact at a resolution of around 70 micrometres per pixel. We compared the post impact μ CT at similar resolutions to highlight the crater volume and structural changes in the material. Fig. 4a. and 4b. show the top and lateral cross section views of an impacted sample from μ CT reconstructions. Higher resolutions are required for further insights into the material microstructure. The impacted area was cut into smaller cubes for μ CT after

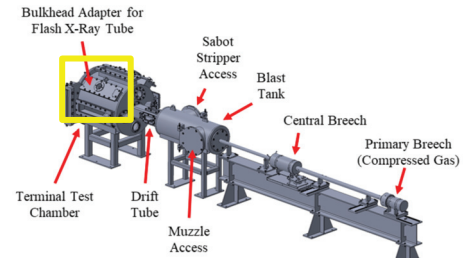


Fig. 3a. Schematic of the HyFIRE facility, with the impact chamber highlighted [8]

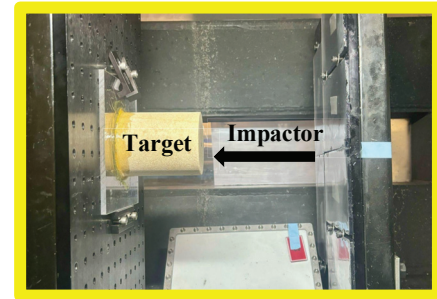


Fig. 3b. Experimental set-up inside HyFIRE

epoxy-impregnation of the impacted sample, as shown in Fig. 4b. These secondary scans provided a resolution of around 25 μ m/ pixel, revealed grain-scale interactions, crack propagation, and changes in porosity around the impact region, highlighted in Fig. 4c and 4d. Our approach aimed to quantify the damage in target material at multiple scales, from the macro level (crater size) down to the microstructural changes such as grain compaction and porosity distributions. These analyses help in understanding the impact response and provide a clearer picture of how the material properties and structure evolved due to the impact.

Table. 1. Experimental conditions for impacts

S.No.	Sandstone target	v_i^a (km/s)	P_{atm}^b (torr)	V^c (mm ³)
1	Bentheimer	1.9	760	833.39
2	Bentheimer	1.9	700	846.38
3	Bentheimer	2.0	700	891.44
4	Nugget	1.9	760	693.28
5	Nugget	1.8	700	418.7
6	Bentheimer	2.0	50	942.19
7	Bentheimer	2.0	50	906.08
8	Nugget	1.9	50	581.63
9	Nugget	1.6	50	404.72

^aImpact velocity. All impacts by 3 mm spherical Aluminium projectiles. ^bAtmospheric Pressure. ^cCrater Volume.

3 Experimental Outcomes

The effect of varying atmospheric pressures and target porosities can be examined through the variation in crater morphologies and impact induced damage in the target. In this analysis, we measured the area, depth and volume of the craters. We assume linear

measurements (e.g., of depth) had an uncertainty equal to the length of a pixel, 25 μm . The planar area encircled by the crater perimeter is considered as the crater area. The deepest point from the impact face of undamaged target is considered as the crater depth. Crater volume is calculated from 3D reconstructions of μCT scans post-impact, listed in Table 1. Our findings demonstrate that atmospheric pressure significantly affects the cratering process in both Bentheimer and Nugget sandstones. For high-porosity Bentheimer sandstone, higher atmospheric pressure leads to smaller crater diameters, while for low-porosity Nugget sandstone, higher atmospheric pressure results in larger craters.

Gault [10] derived empirical formulae for calculating the displaced mass, crater depth, and diameter in dense crystalline rocks. Suzuki et al. [5] demonstrated that the scaling laws are also effective for laboratory impact experiments on sedimentary rocks. The non-dimensional parameter, π_V , for pi-scaling (e.g., Holsapple [11]) of crater volume was obtained as,

$$\pi_V = 10^{-10.061} \left(\frac{\rho_p v_i^2}{2\rho_t} \right)^{1.133} \left(\frac{\rho_t}{\rho_p} \right)^{0.633} \quad (1)$$

where ρ_p , ρ_t and v_i are projectile density, target density, and impact velocity, respectively, for coefficients in cgs units, and,

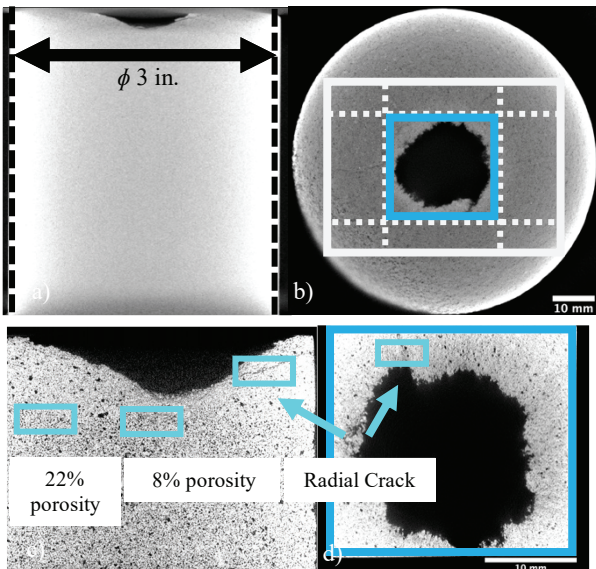


Fig. 4 Crater morphology and target damage observed in micro-CT scans of Bentheimer sandstone post impact at 760 torr. a. Crater cross section. b. Crater plan view. Cubes are cut along the dashed lines for high resolution scans. c. High resolution micro-CT scans show variation in porosity around the impact region. Grain compaction below the crater bed reduces porosity. d. Radial cracks are observed emanating from impact face.

$$\pi_V = \frac{\rho_t V}{m} \quad (2)$$

where m is the mass of the projectile and V is the volume of displaced material, considered as the crater volume here. The predicted crater volumes are then obtained by:

$$V = \frac{m\pi_V}{\rho_t} \quad (3)$$

We acknowledge that Eq. (1) is not dimensionless but was determined through a deliberate modification of a dimensionless form by Suzuki et al. [5]. Fig. 5. shows the relationship between crater volumes and target porosity in our experiments. For comparison, Eq. (3) is shown as a bold line, with ρ_p as 2.7 g/cm³ and ρ_t as 2.1 g/cm³ and 2.4 g/cm³ for Bentheimer and Nugget sandstones, respectively. The values are calculated based on an impact velocity of 2 km/s. Experiments 5 and 9 are not represented because the lower velocities of impact. The deviations from the power law curve reflect the influence of factors beyond porosity, such as target material heterogeneity, and local compaction behaviour not captured in the scaling law.

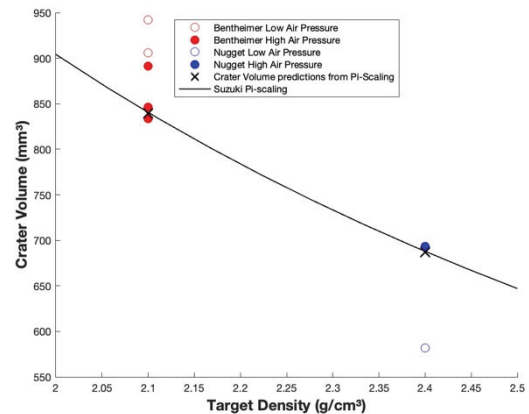


Fig. 5. Comparison of power law with crater volumes observed under different experimental conditions. Impact on Bentheimer sandstones creates smaller craters under higher atmospheric pressures (700- 760 torr) as compared to lower atmospheric pressure (50 torr) but results in larger craters in Nugget sandstones.

3.1 Atmospheric effects on cratering in Bentheimer sandstone

At 50 torr, crater volumes averaging 924 mm³ were formed. As the atmospheric pressure was increased, impact into Bentheimer resulted in smaller crater volumes averaging 857 mm³. While the variation in crater depths wasn't particularly notable for low and high air pressures, much larger crater diameters were formed under lower atmospheric pressures. At 50

torr, the impact craters had an average diameter of 28.54 mm, while at 700-760 torr, the crater diameters averaged 23.45 mm.

Post-impact micro-CT scans revealed that larger cracks formed at higher atmospheric pressures. Fig. 6. shows plan views of Bentheimer impact face under 50 torr and 760 torr. The difference in material fracture can be seen clearly, with large, distinguishable cracks emanating from the impact region for the case of 760 torr. This is consistent with previous findings [4], where presence of interstitial fluids caused more localized deformation, while more compaction was observed in the absence of pore fluids.

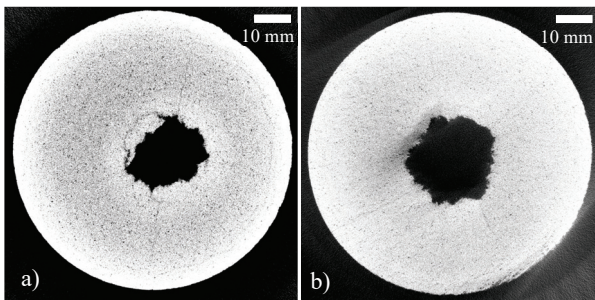


Fig. 6. CT scan of Bentheimer impact face after impact at a. 760 torr, more intergranular cracks observed. b. 50 torr, thinner cracks, more grain compaction leading to porosity changes around impact region.

3.2 Atmospheric effects on cratering in Nugget sandstone

Nugget sandstones show a separate trend in crater morphologies. For 2 km/s impact velocities, the crater volume was observed to be 580 mm³ at 50 torr, which increased to 693 mm³ at 760 torr. Similarly, for impact velocities of 1.6-1.8 km/s, the crater volume increased from approximately 400 mm³ at 50 torr to 420 mm³ at 760 torr. The differences in crater volumes suggest that, unlike Bentheimer sandstone, the interstitial air in Nugget sandstone did not impede the cratering but supported the material excavation during impact. Micro-CT scans show that the craters are flatter under atmospheric pressure but take on a more conical shape in the vacuum. Fig. 7. highlights this variation in crater shapes. Cracks were observed in both low and high atmospheric pressure impacts.

4 Conclusion

The goal of this work is to provide a better understanding of the role of pore spaces and pore fluids in determining the deformation mechanisms in porous rocks during high-velocity impacts. We conducted laboratory experiments on sandstones to investigate the effects of porosity and atmospheric

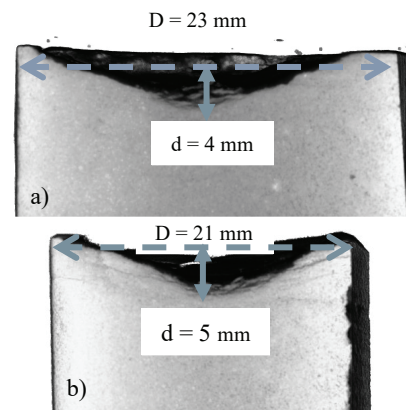


Fig. 7. CT scan of Nugget cross section of a small cube cut around impact region a. 760 torr, larger and flatter crater observed. b. 50 torr, crater is conical.

pressure on the impact behaviour of porous rocks. Our results show that porosity governs the role of interstitial air during impact, affecting both crater size and failure mechanisms. We compared our findings with previous high-velocity crater volume scaling laws to highlight the differences in atmospheric effects on crater sizes for low and high porosity sandstones. Specifically, we propose that in low-porosity rocks, trapped air pressurizes upon impact and enhances grain ejection, increasing crater volume. In contrast, in high-porosity rocks, air can escape readily, reducing this effect and leading to smaller craters. This divergence in behavior provides a mechanistic basis for understanding variability in crater formation across different porosities. Ongoing work includes detailed microstructural analysis of impact damage and the development of numerical models that incorporate porosity and gas-solid interactions.

References

1. Love, S. G., et al. (1993) *Icarus*, 105, 216–224.
2. Baldwin, E. C., et al. (2007) *Meteoritics & Planetary Science*, 42, 1905–1914.
3. Kenkmann, T., et al. (2011) *Meteoritics & Planetary Science*, 46, 890–902.
4. Buhl, Elmar, et al. (2013) *Meteoritics & Planetary Science* 48, 71–86.
5. Suzuki, A., et al. (2012) *JGR: Planets*, 117 (E8).
6. Schultz, Peter H. (1992) *JGR: Planets*, 97 (E1), 975–1005.
7. Royer, John R., et al. (2011) *Europhysics Letters*, 93(2), 28008
8. Hurley, R. C., et al. (2025) *JGR: Solid Earth*, 130 (7).
9. Simpson, Gary, et al. (2019) *15th Hypervelocity Impact Symposium. Vol. 883556, American Society of Mechanical Engineers*.
10. Gault, Donald E. (1973) *The moon*, 6(1), 32–44.
11. Holsapple, Keith A. (1993) *Annual review of earth and planetary sciences. Vol. 21 (A94-10876 01-91)*, p. 333–373.
12. Singh, S. et al. (2025) *56th Lunar and Planetary Science Conference*, Abstract #2196.